Learning Recourse on Instance Environment to Enhance Prediction Accuracy

Lokesh Nagalapatti * **Guntakanti Sai Koushik** **Abir De** **Sunita Sarawagi**
Department of Computer Science and Engineering
IIT Bombay

Abstract

Machine Learning models are often susceptible to poor performance on instances sampled from bad environments. For example, an image classifier could provide low accuracy on images captured under low lighting conditions. In high stake ML applications, such as AI-driven medical diagnostics, a better option could be to provide recourse in the form of alternative environment settings in which to recapture the instance for more reliable diagnostics. In this paper, we propose a model called RECOURSENET that learns to apply recourse on the space of environments so that the recoursed instances are amenable to better predictions by the classifier. Learning to output optimal recourse is challenging because we do not assume access to the underlying physical process that generates the recoursed instances. Also, the optimal setting could be instance-dependent — for example the best camera angle for object recognition could be a function of the object's shape. We propose a novel three-level training method that (a) Learns a classifier that is optimized for high performance under recourse, (b) Learns a recourse predictor when the training data may contain only limited instances under good environment settings, and (c) Triggers recourse selectively only when recourse is likely to improve classifier confidence. We experiment with synthetic and real world datasets to show the efficacy of our proposed approach.

1 Introduction

The performance of any supervised learning model depends strongly on the quality of input instances. However, in practice, instances may be of suboptimal quality when generated in adverse environment settings. For example, even an expressive image classification model may misclassify an image shot at an extreme close-up or at a wrong angle or under poor lighting [13, 28]. Despite large training sizes, such unfavorable instances can deteriorate model performance which can have serious consequences in high stake scenarios like AI guided crop monitoring [21], automatic disease diagnosis from images [22], and AI driven accessibility enhancement for the hearing impaired.

Mitigating the effect of such unfavorable instances entails the design of recourse mechanism to recommend alternative environment *settings* that yield instances revealing the target class. For example, in low cost smartphone based medical diagnosis [22] where imaging is performed by non-experts, such recourse mechanisms can interactively recommend camera settings that yield images optimal for the downstream diagnosis model. Recourse could be particularly useful for healthcare on the edge where users can be prompted to adjust their edge-device settings in real-time to deploy the diagnosis model with higher accuracy. The optimal camera settings however could be label dependent. For example, the best camera angle for recognizing an aeroplane could be different from the angle for recognizing poles.

More formally, the problem that this paper seeks to address is as follows. We have an object z in the physical space (e.g. a crop) with an unknown true label y (e.g. type of disease). Let $\boldsymbol{\beta} \in \mathcal{B}$ be

*nlokeshiisc@gmail.com

36th Conference on Neural Information Processing Systems (NeurIPS 2022).

the environment setting under which we capture a digital representation $\mathbf{x}$ of z to diagnose the label from a downstream classifier $f_\theta(\mathbf{x})$. Our goal during recourse is to recommend an alternative setting $\boldsymbol{\beta}'$ (if any) to the user for getting a different representation $\mathbf{x}'$ of z where $f_\theta(\mathbf{x}')$ is more likely to be correct than $f_\theta(\mathbf{x})$. The above problem is an instance of algorithmic recourse, on which there has been much recent work [30, 29, 23, 8, 32, 11]. These methods recommend recourse actions on the instance space $\mathbf{x}$, which is difficult to realize on raw data for objects such as images and speech. Instead we propose to intervene at the level of the environment which generates the instance via an unknown physical process. We view our contribution under three facets as explained below:

(i) Novel framework for recourse mechanism. We propose RECOURSENET, a trainable recourse mechanism which recommends modified actions to the end user so that, if acted upon the environment, it can generate instances with improved accuracy. RECOURSENET consists of three components: (1) a classifier f_θ, (2) a recourse trigger π (3) a recourse recommender network g_ϕ. Given an instance $(\mathbf{x}, \boldsymbol{\beta})$, the recourse trigger π first decides whether to recommend recourse for $\mathbf{x}$. If so, the recourse recommender g_ϕ suggests an alternative environment $\boldsymbol{\beta}'$. Using these, the user generates a new instance $\mathbf{x}'$, on which f_θ would give the correct label with potentially higher confidence.

(ii) Three level training proposal. The main challenge of RECOURSENET is that we do not assume access to the latent physical process Z that generates an $\mathbf{x}'$ given a $\boldsymbol{\beta}'$ during training. Instead we train with a fixed labeled dataset containing (latent) objects z_i rendered as instances $\{\mathbf{x}_{ij}\}$ under a small but variable set B_i of observed settings $\{\boldsymbol{\beta}_{ij}\}$. We show that direct end-to-end training of a combined likelihood training settles on easy local minima, and fails to provide good recourse. Training them stage wise also is challenging; we list some of these. For f_θ, training on the entire dataset may be suboptimal since instances in poor settings, where recourse will be asked, may mislead decisions on good instances. For g_ϕ, we have no direct supervision of good $\boldsymbol{\beta}$ for a given $(\mathbf{x}_{ij}, \boldsymbol{\beta}_{ij})$. For π, simple heuristics like choosing to recourse examples where f_θ has low confidence does not guarantee improved accuracy. Our training strategy employs careful scheduling and decoupling of the training of the three modules via proxy functions. This achieves substantial gains over simple end-to-end training and existing methods of training classifiers with data selection based purely on noise [20, 2, 5, 12, 14, 17, 24, 31].

(iii) Characterization of recourse conditions. We provide theoretical characterizations to identify the circumstances under which recourse will enhance prediction accuracy. Specifically, we show that given an instance $\mathbf{x}$, if the recourse recommender suggests a modified environment that is close to at least one of the training environments resulting in an improved accuracy, then the recourse is beneficial. Moreover, if there exists some environment which improves the accuracy by a substantial margin, then even a modestly calibrated recourse recommender can lead to improved accuracy.

2 Related work

Our work is closely related to (i) Algorithmic recourse, (ii) Learning with triage and (iii) Machine learning with environment perturbation.

Algorithmic recourse: In recent years, there is an increasing interest in designing recourse on the instance space [30, 29, 23, 8, 32, 11, 25, 9] for a wide variety of applications. For example [30, 29] aim to improve fairness; [15, 7, 10] aim to train the models so that the predicted output is preserved under strategic perturbation of the instance space. Another line of work called strategic classification [7, 15, 10] deals with applying causal interventions to instances. However, these work learn the recourse action on the instance space, whereas, our goal is to design recourse action on the observed environment. An additional challenge in our setting is that the impact of the environment on the instance is latent and we do not assume presence of enough labeled data to learn a generative model for complex real-world instances under different environments.

Learning with triage: A recent line of work [20, 2, 5, 12, 14, 17, 24, 31] aims to learn when to outsource a subset of instances to human and assign the rest of the examples to machine so that machine and human together achieve superior performance than what they would have achieved independently. However, in our problem, humans do not participate in prediction task but they only generate new instances under the recommended environments.

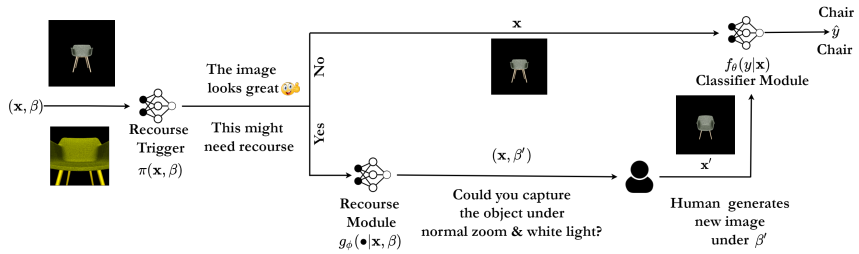

Figure 1: Architecture of Proposed Approach. The chair image on the top does not need recourse but the bottom image obtains the correct label only after recourse.

Machine learning under environment perturbations: Machine learning models are sensitive to environments under which data is generated [13, 28]. For example [13], show that simple parametric perturbations on the Shapenet dataset can flip class labels. In another related work [18] suggests interventions on the environment using policy gradients to train a recourse model. However, they assume the availability of a human through out the training loop to generate data in an on-demand basis. We make no such assumptions and train with a fixed labeled dataset.

3 Proposed approach

In this section, we first formally present our problem, present our training methodology, and then theoretically characterize the settings under which recourse is possible.

Problem formulation Let $\mathcal{Z}$ denote a space of objects, $\mathcal{B}$ denote a space of environment settings which could be real-valued or discrete or mixed, and $\mathcal{X}$ denote a space of instances obtained via a latent physical process $Z : \mathcal{Z} \times \mathcal{B} \to \mathcal{X}$. Given a latent object $z \in \mathcal{Z}$ and an environment setting $\boldsymbol{\beta} \in \mathcal{B}$, we get an instance $\mathbf{x} \in \mathcal{X} = \mathbb{R}^{d_x}$ *i.e.*, $\mathbf{x} = Z(z, \boldsymbol{\beta})$. Each object z has a label $y \in \mathcal{Y}$ with $|\mathcal{Y}| = K$. We are interested in inferring the object's label using a trained classifier f_θ. During training, for each of the latent set of objects $\{z_i\}_{i \in D}$, we are given a true label y_i and for a small set of settings $B_i \subset \mathcal{B}$, we are given instance $\{\mathbf{x}_{ij}\}_{j \in B_i}$. Thus, we view the training data as a set of examples $T = \{y_i, \{\mathbf{x}_{ij}, \boldsymbol{\beta}_{ij}\}_{j \in B_i}\}_{i \in D}$ We use V to index all the examples, *i.e.*, $V = \cup_{i \in D}\{\{i\} \times B_i\}$. As stated earlier, our goal is to design a recourse mechanism that given a representation $\mathbf{x}$ obtained of a latent object z under given settings $\boldsymbol{\beta}$ will recommend an alternative $\boldsymbol{\beta}'$ if the resultant $\mathbf{x}' = Z(z, \boldsymbol{\beta}')$ is expected to yield more accurate prediction under f_θ. Note that Z is not accessible to us during training and we assume in this work that it is difficult to learn Z or infer z from the available labeled data T. Our goal instead is to use T to learn both f_θ and the recourse mechanism.

3.1 Training RECOURSENET

RECOURSENET consists of three components:

1. A classifier $f_\theta : \mathcal{X} \times \mathcal{Y} \to [0, 1]$ which aims to capture the likelihood of the label y given an instance $\mathbf{x}$, *i.e.* $f_\theta(y \mid \mathbf{x})$ approximates $\Pr(y \mid \mathbf{x})$.
2. A recourse recommender network $g_\phi : \mathcal{X} \times \mathcal{B} \times \mathcal{B} \to [0, 1]$, that suggests a modified environment $\boldsymbol{\beta}' \sim g_\phi(\bullet \mid \mathbf{x}, \boldsymbol{\beta})$ such that if the user (via Z) were to regenerate a new instance $\mathbf{x}'$ using $\boldsymbol{\beta}'$ the classifier is likely to provide higher accuracy.
3. A recourse trigger network $\pi : \mathcal{X} \times \mathcal{B} \to \{0, 1\}$ which is a binary decision function. Here, $\pi(\mathbf{x}, \boldsymbol{\beta}) = 1$ indicates that we decide to perform recourse on the environment and the $\boldsymbol{\beta}'$ suggested by g_ϕ should be used to regenerate the instance.

Training objective. Given a set of examples with $\{y_i, \{\mathbf{x}_{ij}, \boldsymbol{\beta}_{ij}\}_{j \in B_i}\}_{i \in D}$, we aim to find θ, ϕ and π by solving the following optimization problem:

$$\max_{\theta, \phi, \pi} \sum_{\substack{i \in D \\ j \in B}} \Big[(1 - \pi(\mathbf{x}_{ij}, \boldsymbol{\beta}_{ij})) \log f_\theta(y_i \mid \mathbf{x}_{ij}) + \pi(\mathbf{x}_{ij}, \boldsymbol{\beta}_{ij}) \log f_\theta(y_i \mid Z(z_i, \operatorname{argmax}_{\boldsymbol{\beta}} g_\phi(\boldsymbol{\beta} \mid \mathbf{x}_{ij}, \boldsymbol{\beta}_{ij}))) \Big] \tag{1}$$

$$\text{subject to,} \sum_{i \in D, j \in B} \pi(\mathbf{x}_{ij}, \boldsymbol{\beta}_{ij}) \leq b, \text{ and } \pi(\mathbf{x}_{ij}, \boldsymbol{\beta}_{ij}) \in \{0, 1\} \tag{2}$$

Algorithm 1: GREEDYALGORITHM for training f_θ

Require: Data $T = \{y_i, \{\mathbf{x}_{ij}, \boldsymbol{\beta}_{ij}\}_{j \in B_i}\}$, b

$V = \cup_{i \in D}\{\{i\} \times B_i\}$
$R \leftarrow \emptyset$, $\theta^0(\emptyset) \leftarrow \textsc{Train}(F(\bullet, \emptyset))$
for $k \in [b]$ **do**
  for $(i,j) \in V \backslash R$ **do**
    $\mathcal{L}[(i,j)] = F(\theta^k(R \cup \{(i,j)\}), R \cup \{(i,j)\})$
  $(i^*, j^*) \leftarrow \text{argmax}_{(i,j) \in V \backslash R} \mathcal{L}[(i,j)]$
  $R \leftarrow R \cup \{(i^*, j^*)\}$
  $\theta^{k+1}(R) \leftarrow \textsc{Train}(F(\bullet, R))$
Return $\theta^{k+1}(R)$

Algorithm 2: TrainRECOURSENET

Require: Train data $T = \{y_i, \{\mathbf{x}_{ij}, \boldsymbol{\beta}_{ij}\}_{j \in B_i}\}$, b, δ

$\hat{\theta} \leftarrow \textsc{GreedyAlgorithm}(T, b)$
$\hat{\phi}, f^{\text{CF}} \leftarrow \textsc{RecRecommender}(T, \delta, \hat{\theta})$ `// Eq (8)`
Return $\hat{\theta}, \hat{\phi}, f^{\text{CF}}$

Algorithm 3: RECOURSENET Inference

Require: Test instance $(z, \mathbf{x}, \boldsymbol{\beta})$, Z (human), $\hat{\theta}$, $\hat{\phi}$, f^{CF}

$\hat{\pi} \leftarrow \textsc{RecTrigger}(\mathbf{x}, \boldsymbol{\beta}, \hat{\theta}, \hat{\phi}, f^{\text{CF}})$ `// Eq (9)`
$\hat{y} \leftarrow \text{argmax}_y \big[(1 - \hat{\pi}(\mathbf{x}, \boldsymbol{\beta})) f_{\hat{\theta}}(y|\mathbf{x}) + \hat{\pi}(\mathbf{x}, \boldsymbol{\beta}) f_{\hat{\theta}}(y | Z(z, \text{argmax}_{\boldsymbol{\beta}'} g_{\hat{\phi}}(\boldsymbol{\beta}'|\mathbf{x}, \boldsymbol{\beta})))\big]$
Return $\hat{y}$

Here, b indicates the maximum number of examples which can undergo recourse. The first term in the objective (1) $(1 - \pi(\bullet, \bullet)) \log f_\theta(\bullet \,|\, \bullet)$ accounts for examples that do not need recourse and the second term $\pi(\bullet, \bullet) \log f_\theta(\bullet \,|\, \bullet)$ accounts for those that need recourse. End to end training of the optimization problem (1)— (2) is challenging since we do not have an analytical form of Z and training such a process will be difficult. We propose to train the three components f_θ, g_ϕ, π in a carefully designed three-stage process that we describe next.

Training the classifier f_θ. Training f_θ on the entire training data may be sub-optimal because instances in poor settings would be subject to recourse, and the classifier should instead focus on instances after recourse as the above training objective suggests. For training f_θ first we eschew the involvement of Z and g_ϕ from the training objective (1) by noting that $\pi(\mathbf{x}_{ij}, \boldsymbol{\beta}_{ij}) = 1$ only if $f_\theta(y_i \,|\, Z(z_i, \text{argmax}_{\boldsymbol{\beta}} g_\phi(\boldsymbol{\beta} \,|\, \mathbf{x}_{ij}, \boldsymbol{\beta}_{ij}))) \geq f_\theta(y_i \,|\, \mathbf{x}_{ij})$. Therefore, we replace the term $Z(z_i, \text{argmax}_{\boldsymbol{\beta}} g_\phi(\boldsymbol{\beta} \,|\, \mathbf{x}_{ij}, \boldsymbol{\beta}_{ij}))$ with some instance $(\mathbf{x}_{ir}, \boldsymbol{\beta}_{ir})$ for some $r \in B_i$ of the same object z_i such that the predicted classification accuracy on $\mathbf{x}_{ir}$ is better than the original instance $\mathbf{x}_{ij}$ by a certain margin Δ. Specifically, given $(\mathbf{x}_{ij}, \boldsymbol{\beta}_{ij})$, we first define $\text{Rec}_\Delta(\theta, \mathbf{x}_{ij}, y_i)$ as the set of environments which would improve the log-likelihood of the gold label by at least a margin Δ *i.e.*,

$$\text{Rec}_\Delta(\theta, \mathbf{x}_{ij}, y_i) = \{\boldsymbol{\beta}' \in B_i \mid \log f_\theta(y_i \,|\, Z(z_i, \boldsymbol{\beta}')) > \log f_\theta(y_i \,|\, \mathbf{x}_{ij}) + \Delta\} \tag{3}$$

and then we pose the following training problem to learn θ.

$$\max_{\theta, \pi} \sum_{\substack{i \in D \\ j \in B_i}} \left[(1 - \pi(\mathbf{x}_{ij}, \boldsymbol{\beta}_{ij})) \log f_\theta(y_i \,|\, \mathbf{x}_{ij}) + \pi(\mathbf{x}_{ij}, \boldsymbol{\beta}_{ij}) \max_{\boldsymbol{\beta}_{ir} \in \text{Rec}_\Delta(\theta, \mathbf{x}_{ij}, y_i)} \log f_\theta(y_i \,|\, \mathbf{x}_{ir}) \right]$$

$$\text{subject to,} \sum_{i \in D, j \in B_i} \pi(\mathbf{x}_{ij}, \boldsymbol{\beta}_{ij}) \leq b, \text{ and } \pi(\mathbf{x}_{ij}, \boldsymbol{\beta}_{ij}) \in \{0, 1\}. \tag{4}$$

Since our budget is limited, one needs to spend it on only those instances which not only suffer from poor accuracy, but can also lead to new instances that promote f_θ to predict the correct label. The presence of a non-zero margin Δ ensures such a condition. In Section 3.2, we provide the conditions under which such a recourse set will exist.

Given $\pi(\mathbf{x}_{ij}, \boldsymbol{\beta}_{ij}) \in \{0, 1\}$, we first define the set $R = \{(i,j) \,|\, \pi(\mathbf{x}_{ij}, \boldsymbol{\beta}_{ij}) = 1\}$. Then, we can write the objective (4) as

$$\max_{\theta, R: |R| \leq b} F(\theta, R) = \sum_{(i,j) \notin R} \log f_\theta(y_i \,|\, \mathbf{x}_{ij}) + \sum_{(i,j) \in R} \max_{\boldsymbol{\beta}_{ir} \in \text{Rec}_\Delta(\theta, \mathbf{x}_{ij}, y_i)} \log f_\theta(y_i \,|\, \mathbf{x}_{ir}) \tag{5}$$

which gives us the problem of subset selection in conjunction with parameter estimation. Note that the involvement of R as an optimization variable renders the above problem challenging even if $\log f_\theta(y \,|\, \mathbf{x})$ is concave in θ. Thus, we resort to a greedy algorithm [19, 5, 16, 33] to solve this optimization problem (summarized in Algorithm 1). It is an iterative routine, which picks up an instance $(\mathbf{x}_{ij}, \boldsymbol{\beta}_{ij}, y_i)$ at every iteration which will maximize the training objective. Given an update R at step $k \leq b$, it chooses a candidate instance (i,j) which maximizes $F(\theta^k(R \cup \{(i,j)\}), R \cup \{(i,j)\})$, where $\theta(S) = \max_\theta F(\theta, S)$. We would like to highlight that, by definition of the set Rec_Δ, inclusion of (i,j) in R either improves the log-likelihood or keeps it at the same value obtained in the previous iteration. Formally, we can say that $F(\theta^{k+1}(R \cup \{(i,j)\}), R \cup \{(i,j)\}) \geq F(\theta^k(R), R)$.

Learning g_ϕ. Objective (1) is non-differentiable in ϕ because of the $\operatorname{argmax}_{\boldsymbol{\beta}} g_\phi(\bullet)$ input to f_θ and the unknown Z. We first get rid of the argmax term via the following surrogate:

$$\operatorname*{argmax}_{\phi} \sum_{\substack{i\in D, j\in B_i \\ \pi(\mathbf{x}_{ij})=1}} \log f_\theta(y_i \mid Z(z_i, \operatorname{argmax}_{\boldsymbol{\beta}} g_\phi(\boldsymbol{\beta} \mid \mathbf{x}_{ij}, \boldsymbol{\beta}_{ij}))) \approx \operatorname*{argmax}_{\phi} \sum_{\substack{i\in D, j\in B_i \\ \pi(\mathbf{x}_{ij})=1}} \max_{\boldsymbol{\beta}} \log\left[f_\theta(y_i \mid Z(z_i, \boldsymbol{\beta}))\, g_\phi(\boldsymbol{\beta} \mid \mathbf{x}_{ij}, \boldsymbol{\beta}_{ij})\right] \tag{6}$$

Next we account for the unknown Z by partitioning all examples in D into two groups — the set D_δ which contains groups with at least one instance where good $\boldsymbol{\beta}$s are available (*i.e.*$\max_r f_\theta(y_i|\mathbf{x}_{ir}) > 1-\delta$), and the remaining objects $D - D_\delta$ where no good instances are available. For the instances in $D - D_\delta$ we need to find a good $\boldsymbol{\beta}$ to train g_ϕ. For this we first estimate a function $f^{\text{CF}}(y_i|\mathbf{x}_{ij}, \boldsymbol{\beta})$ that estimates the confidence $f_\theta(y_i|Z(z_i, \boldsymbol{\beta}))$. That is, it approximates f_θ when $\boldsymbol{\beta}_{ij}$ is replaced by $\boldsymbol{\beta}$ for the i-th object. We estimate this quantity as the average classifier accuracy on objects with similar labels and under settings $\boldsymbol{\beta}$. In general, for continuous $y, \boldsymbol{\beta}$ this can be fit as a regression problem. For discrete $y, \boldsymbol{\beta}$, simple fractional estimates were found adequate in our experiments. We compute these estimates by defining the following counterfactual:

$$f^{\text{CF}}(y \mid \mathbf{x}, \boldsymbol{\beta}) = \frac{\sum_{(i,j)\in V} \mathbb{I}[y_i = y, \boldsymbol{\beta}_{ij} = \boldsymbol{\beta}] f_{\hat{\theta}}(y_i = y \mid \mathbf{x}_{ij})}{\sum_{(i,j)\in V} \mathbb{I}[y_i = y, \boldsymbol{\beta}_{ij} = \boldsymbol{\beta}]} \tag{7}$$

where $\mathbb{I}[\bullet]$ is an indicator function and $\hat{\theta}$ is the output of Algorithm 1. With these two terms, we maximize the following objective:

$$\max_{\phi} \sum_{\substack{i\in D_\delta \\ j\in B_i}} \max_{r\in B_i} \log\left[f_\theta(y_i \mid \mathbf{x}_{ir})\, g_\phi(\boldsymbol{\beta}_{ir} \mid \mathbf{x}_{ij}, \boldsymbol{\beta}_{ij})\right] + \sum_{\substack{i\notin D_\delta \\ j\in B_i}} \log g_\phi\left(\operatorname{argmax}_{\boldsymbol{\beta}} f^{\text{CF}}(y_i \mid \mathbf{x}_{ij}, \boldsymbol{\beta}) \mid \mathbf{x}_{ij}, \boldsymbol{\beta}_{ij}\right) \tag{8}$$

Computation of π. Our training objective (1) suggests that $\pi(\mathbf{x}_{ij}, \boldsymbol{\beta}_{ij}) = 1$ only if $f_\theta(y_i \mid \mathbf{x}_{ij}) < f_\theta(y_i \mid \mathbf{x}'_{ij} = Z(z_i, \boldsymbol{\beta}'_{ij}))$ where $\boldsymbol{\beta}'_{ij} = \operatorname{argmax}_{\boldsymbol{\beta}} g_{\hat{\phi}}(\boldsymbol{\beta} \mid \mathbf{x}_{ij}, \boldsymbol{\beta}_{ij}))$. Since the recourse budget is limited, we cannot obtain $\mathbf{x}'_{ij}$ for all instances to compute π. Therefore, in practice, we use $f^{\text{CF}}(\bullet|\mathbf{x}_{ij}, \boldsymbol{\beta}'_{ij})$ as a proxy for $f_\theta(\bullet \mid \mathbf{x}'_{ij} = Z(z_i, \boldsymbol{\beta}'_{ij}))$. Specifically, we set

$$\pi(\mathbf{x}_{ij}, \boldsymbol{\beta}_{ij}) = \mathbb{I}[f^{\text{CF}}(y_{\max} \mid \mathbf{x}_{ij}, \boldsymbol{\beta}'_{ij}) > f_{\hat{\theta}}(y_{\max} \mid \mathbf{x}_{ij})] \text{ where } y_{\max} = \operatorname*{argmax}_{y} f_{\hat{\theta}}(y \mid \mathbf{x}_{ij}) \tag{9}$$

We call our overall training method as RECOURSENET, which is summarized in Algorithm 3.

3.2 Theoretical Analysis

In this section we present the conditions on θ, ϕ, π under which RECOURSENET will be successful in providing recourse. The proofs of the propositions are given in Appendix B.

Proposition 1 *Assume that Z is $L_{\boldsymbol{\beta}}$-Lipschitz with respect to $\boldsymbol{\beta}$, the model $\log f_\theta(y \mid \mathbf{x})$ is L_x-Lipschitz with respect to $\mathbf{x}$. Given $i \in D$ and $j \in B_i$, if the set $\operatorname{Rec}_\Delta(\theta, \mathbf{x}_{ij}, y_i)$ is non-empty and the recourse network g_ϕ gives a modified $\boldsymbol{\beta}'_{ij}$ such that $||\boldsymbol{\beta}'_{ij} - \boldsymbol{\beta}|| \le \epsilon$ for some $\boldsymbol{\beta} \in \operatorname{Rec}_\Delta(\theta, \mathbf{x}_{ij}, y_i)$, then, for $\Delta > tL_xL_{\boldsymbol{\beta}}\epsilon$ with $t > 1$ we have:*

$$\log f_\theta(y_i \mid Z(z_i, \boldsymbol{\beta}'_{ij})) > \log f_\theta(y_i \mid \mathbf{x}_{ij}) + (1 - 1/t)\,\Delta \tag{10}$$

The above proposition suggests that as long as $g_\phi(\bullet \mid \mathbf{x}_{ij}, \boldsymbol{\beta}_{ij})$ is close to some $\boldsymbol{\beta} \in \operatorname{Rec}_\Delta(\theta, \mathbf{x}_{ij}, y_i)$, then the accuracy provided by the classifier f_θ improves. One of the key assumption of this proposition is the non-emptiness of $\operatorname{Rec}_\Delta(\theta, \mathbf{x}_{ij}, y_i)$. In the following proposition, we find the requirements for such conditions in terms of the true classifier f_{θ^*}.

Proposition 2 *Let us assume that the true conditional distribution of y given $\mathbf{x}$ is f_{θ^*}, $\log f_\theta(y \mid \mathbf{x})$ is L_θ-Lipschitz w.r.t. θ and $||\theta - \theta^*|| \le \delta$. Given $i \in D$ and $j \in B_i$, if $\operatorname{Rec}_{\Delta_0}(\theta^*, \mathbf{x}_{ij}, y_i)$ is non-empty for some $\Delta_0 > 2L_\theta\delta$, then $\operatorname{Rec}_\Delta(\theta, \mathbf{x}_{ij}, y_i)$ is non-empty for $\Delta < \Delta_0 - 2L_\theta\delta$. Moreover, if the recourse network g_ϕ gives us a modified $\boldsymbol{\beta}'_{ij}$ such that $||\boldsymbol{\beta}'_{ij} - \boldsymbol{\beta}|| \le \epsilon$ for some $\boldsymbol{\beta} \in \operatorname{Rec}_\Delta(\theta, \mathbf{x}_{ij}, y_i)$, then, for $\Delta_0 > 2L_\theta\delta + tL_{\boldsymbol{\beta}}L_x\epsilon$ with $t > 1$ we have:*

$$\log f_\theta(y_i \mid Z(z_i, \boldsymbol{\beta}'_{ij})) > \log f_\theta(y_i \mid \mathbf{x}_{ij}) + (1 - 1/t)(\Delta_0 - 2L_\theta\delta) \tag{11}$$

Dataset	#Train objects ($\|D\|$)	#Renderings ($\|B_i\|$)	Environment ($\mathcal{B}$)	#Classes $\|\mathcal{Y}\|$	#Test objects
Synthetic	1200	8	6 dimensional bit-mask	4	200
Shapenet-Large	2500	4	`(view, zoom level, light color)`	10	800
Shapenet-Small	2500	2	`(view, zoom level, light color)`	10	800
Speech Commands	2000	5	`(pitch, speed, noise)`	20	60
Skin Lesion	1400	4	`(zoom, illumination, contrast)`	7	70

Table 2: Summary of datasets used. #Train objects denotes the number of (latent) objects that are available in the dataset. #Renderings denotes the number of environment settings under which each such object z_i is rendered. Environment column denotes the different parameters that can be instantiated to render $\mathbf{x}$ from z. Finally, #Test objects denotes the number of (latent) objects available in the test dataset. Unlike train, we render each test object under all possible environments $\boldsymbol{\beta} \in \mathcal{B}$.

4 Experiments

In this section, we experiment with several datasets to show that RECOURSENET's training strategy outperforms existing methods or simpler alternatives. Our experiments are designed to answer the following research questions through empirical evaluations:

1. In the training of f_θ, what is the impact of subsetting the training set when compared with default alternatives like training on all available labeled data.
2. In deciding when to trigger recourse, how effective is our method, in contrast to just asking recourse on low confidence examples?
3. In training the recourse recommender, how important was it distinguish between objects with and without good $\boldsymbol{\beta}$s? During inference, how important is it to make instance specific recourse recommendations instead of a single ideal beta?

We could not find any existing benchmark that records different environment settings under which objects are rendered. Thus we generate datasets that admit causal relationship across $\mathbf{x}, \boldsymbol{\beta}, z$ and y as follows: we first sample a class label from the class prior $y \sim \Pr(\bullet)$ and then we choose B_i settings by sampling $\boldsymbol{\beta}$s drawn from a $\Pr(\boldsymbol{\beta} \mid y)$. Finally we generate $\mathbf{x}$ under the B_i chosen environments. We generate 4 datasets of varying complexities as shown in the Table 2.

Shapenet-Large Shapenet consists of three dimensional models of many kinds of objects that can be mapped into two dimensional pixel maps under various environments [3]. Each environment $\boldsymbol{\beta}$ represents the camera settings provided by `(view, zoom level, light color)`. We select $|\mathcal{Y}| = 10$ classes and draw 250 objects from each class to obtain a total of $|D| = 2500$ objects. For each object, we draw $B_i = 4$ different $\boldsymbol{\beta}$s from a set of $|\mathcal{B}| = 9$ possible camera settings and render them under these settings. Among the four environments, we ensure that each z_i contains a $\boldsymbol{\beta}$ that renders it properly with a probability 0.8. To make the task challenging, we corrupt the rendered $\mathbf{x}_{ij}$ using various kinds of noise from the image corruptions library[2]. In particular, we corrupt $\mathbf{x}_{ij}$ if $\boldsymbol{\beta}_{ij}$ is not a good choice for z_i so as to make learning of such settings difficult for f_θ.

Shapenet-Small. This dataset differs from Shapenet-Large in the number of environments under which each object is rendered. Among the two environments, each z_i contains a good $\boldsymbol{\beta}$ with probability 0.6. This dataset is more challenging than Shapenet-Large because of scarcity in the number of objects that contain atleast one $\mathbf{x}_{ij}$ that produces good accuracy. This makes the objective (6) difficult to learn. Here also we add noise to $\mathbf{x}_{ij}$ in a manner similar to Shapenet-Large. The test set for both Shapenet-Large and Shapenet-Small is same, and contains 80 objects per class; each of them rendered under all 9 camera settings $\boldsymbol{\beta}$ thus contributing to 7200 images.

Speech Commands Dataset. This dataset consists of textual commands that can be converted to speech under different environments $\boldsymbol{\beta}$ defined by `(pitch, speed, noise)` sampled from $\mathcal{B}$ with $|\mathcal{B}| = 60$. We select $|\mathcal{Y}| = 20$ commonly used Alexa commands and render them to speech signals with a frame width of 0.5 seconds using Google text to speech library [3]. These speech signals are then processed into 2D mel spectrograms [27]. In particular, the training dataset consists of 2000 z_i rendered under $|B_i| = 5$ environments each thereby contributing to 10000 samples. The test set contains 200 z_is rendered under all 60 $\boldsymbol{\beta}$s thereby containing 12000 speech samples.

[2] `https://github.com/bethgelab/imagecorruptions`

[3] `https://cloud.google.com/text-to-speech`

Training Data	Shapenet-Large	Shapenet-Small	Speech-Commands	Skin-Lesion
Full-data (Baseline)	71.93 ± 0.63	62.97 ± 0.80	51.85 ± 1.08	56.42 ± 0.80
One-shot subsetting	72.63 ± 0.54	65.55 ± 1.11	54.66 ± 1.2	60.89 ± 1.11
Iterative greedy (Ours)	$\mathbf{77.14 \pm 0.63}$	$\mathbf{74.13 \pm 1.10}$	$\mathbf{65.76 \pm 1.44}$	$\mathbf{68.62 \pm 0.90}$

Table 3: Comparing classification accuracy under different strategies for subsetting data for training f_θ at 100% recourse. The table shows mean $\pm$ one std. deviation of accuracies obtained over 5 seeds.

Skin-Lesion Dataset This dataset consists of images of skin captured using smartphone and the task is to classify among seven different skin conditions ($|\mathcal{Y}| = 7$). The dataset is taken from Kaggle [4] and we synthetically generate 9 different environments ($|\mathcal{B}| = 9$) where each environment is defined by `(zoom, illumination, contrast)`. The training dataset contains 1400 objects z_i rendered under $|B_i| = 4$ environments each and the test dataset contains 70 objects rendered under all 9 environments.

Further details about dataset preparation and results on synthetic datasets are provided in Appendix C.

Models and Hyper-parameters. We use the same model architecture and hyper-parameters across datasets. We used Adam optimizer with default learning rate of 10^{-3} to optimize all our objectives. The architecture for f_θ is a Resnet18 model trained from scratch. We use budget $b = 1000$ but to avoid training the model iteratively b times, we select 10 instances into R at line 5 of algorithm 1 per iteration. For g_ϕ too we train a Resnet18 model from scratch. We obtain 512-dimensional embedding for $\boldsymbol{\beta}$ as an average of embeddings of its individual components which are trained end-to-end. We concatenate the embeddings of $\boldsymbol{\beta}$ with last layer embeddings of $\mathbf{x}$ from Resnet18 to obtain the input embedding which is then fed to a 3-layered neural network that predicts the recourse $\boldsymbol{\beta}$. We learn g_ϕ using the objective 8 where the D_δ is computed by sorting the minimum group loss ($min_j \mathcal{L}[(i,j)]$) and then selecting the first few groups that produce least min loss into the set D_δ. The first few are chosen so that the average confidence $f_\theta(y_i|\mathbf{x}_{ij}, \boldsymbol{\beta}_{ij})$ of examples in D_δ has the maximum gap with corresponding average in $D - D_\delta$.

RQ1: Impact of subsetting the training data in learning f_θ We compare our iterative greedy proposal to train f_θ with two other baselines as follows:

1. **Full data:** Here we train f_θ over the entire training dataset.
2. **One-shot subsetting:** Here we subset all b examples at once unlike our iterative algorithm 1. *i.e.* we compute $\mathcal{L}(i,j)$ for all samples given $\theta^0(\emptyset)$ and choose the ones that incur *top-b* values into R and then maximize $F(\bullet, R)$ to obtain $\hat{\theta}$.

Table 3 shows the recourse accuracy of f_θ at 100% recourse when learned under these three different training strategies. For all three methods we use g_ϕ trained using our objective (8) to obtain recourse recommendations. We observe that our iterative greedy algorithm to train f_θ consistently outperforms the model trained with the entire data. This establishes the importance of training classifiers differently when recourse is an option. A classifier that is trained only on instances with 'good' environment settings is more suitable for classification under recourse, even in data hungry deep learning models. Simply subsetting by removing the worst b instances is significantly worse than our iterative algorithm.

RQ2: Evaluating our method of triggering recourse We compare our proposal for f_θ and π with four other baselines and the first two are adapted from the work of [24].

1. **Score based recourse trigger:** Here, we train f_θ on entire training data. Then during inference, given a budget b, we seek recourse on the least b confident predictions of f_θ.
2. **Full automation based recourse trigger:** Here also, we train f_θ on entire training data. Then for recourse trigger, we learn an error predictor trained on the loss incurred by the classifier on training examples. During inference, for a budget b, we seek recourse on those examples that incur the b highest predicted losses. Details about the neural architecture of the error predictor is provided in Appendix E.
3. **Random trigger:** We train f_θ on entire dataset and apply recourse on instances selected randomly.

[4] `https://www.kaggle.com/code/kmader/deep-learning-skin-lesion-classification/notebook`

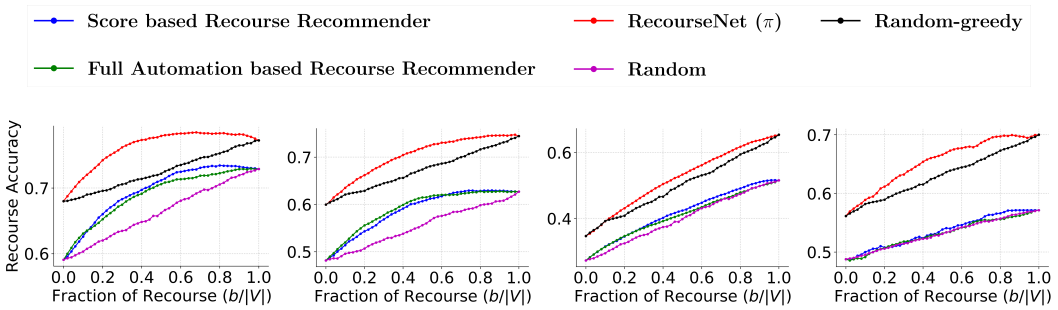

(a) Shapenet-Large (b) Shapenet-Small (c) Speech Commands (d) Skin-Lesion

Figure 4: Variation of classification accuracy after recourse against the budget b, *i.e.*, the maximum number of instances selected for recourse.

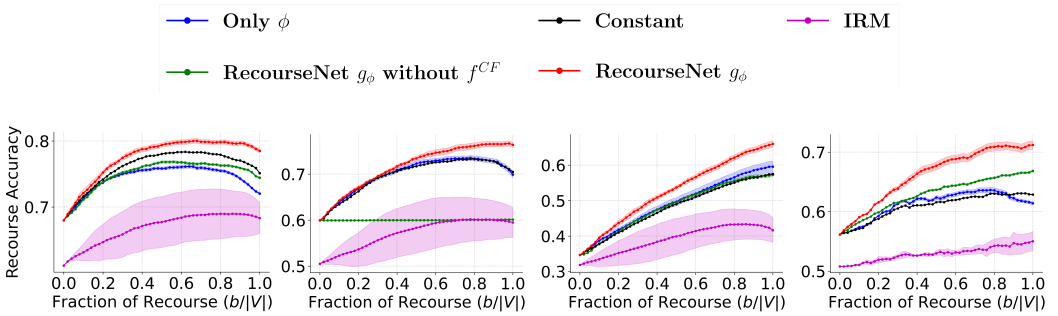

(a) Shapenet-Large. (b) Shapenet-Small. (c) Speech Commands. (d) Skin-Lesion.

Figure 5: Variation of classification accuracy after recourse against the budget b, *i.e.*, the maximum number of instances selected for recourse. The figures show mean recourse accuracy $\pm$ one std. deviation obtained over five seeds.

4. **Random-greedy trigger:** Here we train f_θ using our greedy algorithm 1 and then apply recourse on instances selected randomly.

Figure 4 summarizes the comparison of recourse trigger π against the baselines. Unlike our greedy algorithm, methods that propose full training for f_θ are inferior at 0% recourse. The steepness in the recourse accuracy for our proposed π is more in comparison to other baselines because it prioritizes recourse not just the instances that suffer from poor accuracy for recourse but also the ones that respond better to recourse by means of modelling the expected recourse accuracy. Our method suggests recourse only when the expected gains that we calculate using f^{CF} is positive, and performs much better than methods based purely on current classifier confidence or an estimate of the confidence. We see that both the random baselines perform much worse and follows the expected linear trend of recourse accuracy as we increase the recourse budget. These results establish the impact of our method of triggering response.

RQ3: Evaluating training methods of recourse recommendation g_ϕ We compare our g_ϕ against four other methods as follows.

1. **Only** ϕ**:** This model takes a form similar to g_ϕ and learns to recourse the instances (i, j) that incur top 50% losses in the training data to $\boldsymbol{\beta}_{ir}$ where r is obtained from $\text{argmax}_r\, f_\theta(y_i \,|\, \mathbf{x}_{ir})$.
2. **RecourseNet without** f^{CF}**:** This model trains g_ϕ using the objective (6).
3. **Constant:** This method entails a constant $\boldsymbol{\beta}$ recommendation independent of the features $(\mathbf{x}, \boldsymbol{\beta})$. We select constant $\boldsymbol{\beta}$ as the one that achieves the best training accuracy.
4. **IRM:** In this baseline, instead of g_ϕ we learn networks that estimate accuracy of an input $\mathbf{x}_{ij}$ on a counterfactual setting $\boldsymbol{\beta}$ using ideas from Invariant Risk Minimization literature. We extract representations of input $(\mathbf{x})$ by fine tuning a Resnet18 model with pre-trained Imagenet weights. This forms the Φ network of IRMv1 objective in [1]. The representations are multiplied with a scalar $w = 1$ and then concatenated with representation of the counterfactual environment $\boldsymbol{\beta}$ for which we want to estimate the accuracy. We use a linear layer to embed the environments $(\boldsymbol{\beta})$.

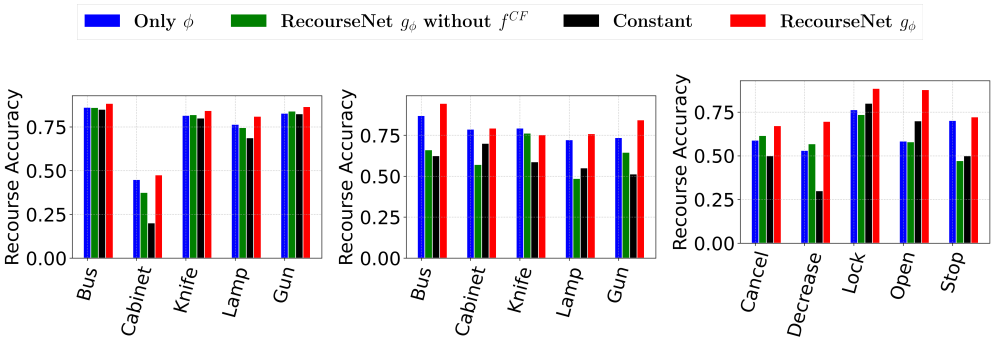

(a) Shapenet-Large (b) Shapenet-Small (c) Speech Commands

Figure 6: Accuracy of different recourse recommenders for different classes.

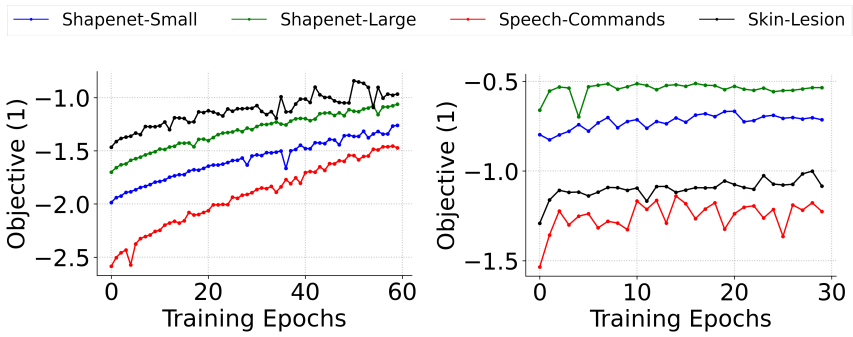

(a) Stability f_θ (b) Stability g_ϕ

Figure 7: Stability of our proposals in solving 1

The concatenated representations are then fed to a fully connected network that aims to predict the classifier's confidence ($f_\theta(y|\mathbf{x})$) on the examples. For Triage, since these methods directly model the counterfactual accuracy $P(y|\mathbf{x}, \boldsymbol{\beta})\ \forall \boldsymbol{\beta}$, we use these predicted values in place of our prior f^{CF} term in Eq. (9). The classifier is trained on the full data.

The first three baselines are designed to perform an ablation study of our proposal, including assessing the importance of finding the objects that have no good $\boldsymbol{\beta}$ and thereby including them in the set $D - D_\delta$ in the g_ϕ objective (8). The results presented in Figure 5 shows the following observations. (1) Only ϕ model performs poorly on Shapenet-Large and performs on par with Constant method on other datasets. Because many groups do not have $\boldsymbol{\beta}$ that produce good accuracy, *Only* ϕ receives noisy supervision during training. (2) RECOURSENET without f^{CF} achieves a decent fit on Shapenet-Large and Specch datasets but fails miserably on the Shapenet-Small dataset. Because Shapenet-Small has $|B_i| = 2$, we can see that 50% examples force the recourse recommender to predict the input $\boldsymbol{\beta}$ as is under the joint objective (6). This renders identity function as a strong local maxima which the model struggles to avoid during training. This brittleness of RECOURSENET without f^{CF} to objects with no good $\boldsymbol{\beta}$ motivates the need for our current objective 8. (3) The supervision provided by the f^{CF} term in our g_ϕ objective (8) guides instances in the set $D - D_\delta$ and thus achieves better recourse accuracy. (4) The IRM method is difficult to train as seen by the large variance, and performs poorly. This method does not sufficiently exploit the fact that the training data includes multiple views of the same object. Also, it suffers because the classifier is trained on full data. (5) One good competitor to our g_ϕ across the datasets is constant prediction which brings us to the other half of RQ3 – Is an instance independent constant $\boldsymbol{\beta}$ recourse recommendation always advisable?

We try to answer this question by probing the average error incurred by these methods for each class. Figure 6 summarizes the results for 5 classes which shows that unlike baselines, our g_ϕ garners modest to best accuracy across classes consistently. The performance of constant method in the Shapanet datasets can be attributed to the fact that many objects in it admit a unique good $\boldsymbol{\beta}$. However, this is not the case in the speech dataset because we found no one $\boldsymbol{\beta}$ to dominate in performance across classes. As a result, the recourse accuracy suffers in the speech dataset with constant $\boldsymbol{\beta}$ prediction. Thus we conclude by saying that it is always good to make instance specific recourse recommendations.

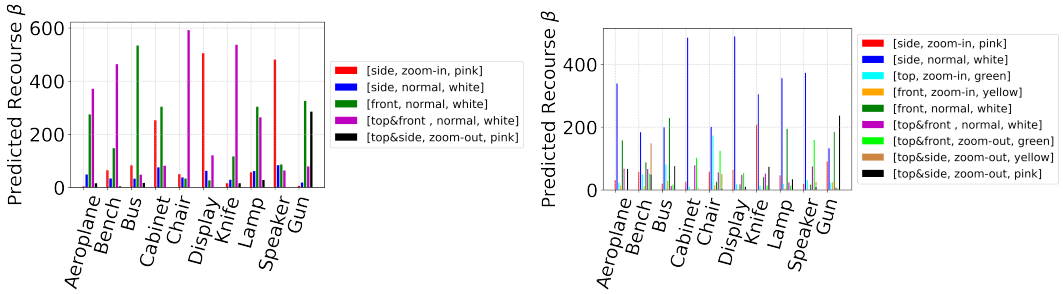

(a) Shapenet-Large

(b) Shapenet-Small

Figure 8: This figure shows the histogram of the counts of different $\boldsymbol{\beta}$s predicted against each class for Shapenet-Large and Shapenet-Small datasets.

5 Stability of our proposals in solving the overall objective 1

In Figure 7(a) we plot the value of the overall objective 1 through the different stages of the f_θ training algorithm and in Figure 7(b) we plot for the second g_ϕ training phase. In both cases we observe that the value of the overall objective increases even though the two stages are not directly solving for Equation 1. This provides empirical evidence about the stability of our method.

Now, we discuss about the details on how we evaluated the overall objective in these two stages. For the f_θ training phase we evaluate the objective using R and $\text{Rec}_\Delta(\theta^k, \mathbf{x}_{ij}, y_i)\}$ as proxies for π and g_ϕ which have not yet been trained. For the g_ϕ training since π is not available, we assume full recourse and focus on the impact of $\boldsymbol{\beta}$s predicted by g_ϕ on recourse objective.

6 Predicted Environments by g_ϕ

In this experiment, we plot the counts of different $\boldsymbol{\beta}$s predicted by our g_ϕ model against each class for Shapenet-Large and Shapenet-Small datasets. For Shapenet-Large, we see that the recourse recommender never predicted 4 out of $9\boldsymbol{\beta}$s for any class and thus those bars are excluded from the figure 8(a). However, this is not the case for Shapenet-Small and hence all $9\boldsymbol{\beta}$s are included.

7 Conclusions

In this paper, we proposed RECOURSENET that aims to make recourse recommendations to instances that are sampled from poor environments. RECOURSENET has three components: (1) classifier f_θ, (2) Recourse recommender g_ϕ and (3) Recourse trigger π. We learn these components using a novel three level training objective without having to model the latent physical generator Z. Moreover, our theoretical results assure that under mild conditions, recourse is beneficial. These results in effect, press the need for recourse in order to obtain quality predictions from a model. The experiments on synthetic and real-world datasets show that our method outperforms several baselines.

Our work opens up many areas of future work. It would be interesting to extend RECOURSENET to regimes where the space of environment variable $\boldsymbol{\beta}$s can be continuous. Also, multiple views of a test object collected during recourse could be exploited to improve future decisions.

8 Acknowledgements

Lokesh is supported by the Prime Minister Research Fellowship, Government of India.

References

[1] Martin Arjovsky, Léon Bottou, Ishaan Gulrajani, and David Lopez-Paz. Invariant risk minimization. *arXiv preprint arXiv:1907.02893*, 2019.

[2] Gagan Bansal, Besmira Nushi, Ece Kamar, Eric Horvitz, and Daniel S. Weld. Optimizing AI for Teamwork. In *AAAI*, 2021.

[3] Angel X. Chang, Thomas Funkhouser, Leonidas Guibas, Pat Hanrahan, Qixing Huang, Zimo Li, Silvio Savarese, Manolis Savva, Shuran Song, Hao Su, Jianxiong Xiao, Li Yi, and Fisher Yu. Shapenet: An information-rich 3d model repository, 2015.

[4] Zachary Charles and Dimitris Papailiopoulos. Stability and generalization of learning algorithms that converge to global optima. In *International conference on machine learning*, pages 745–754. PMLR, 2018.

[5] Abir De, Paramita Koley, Niloy Ganguly, and Manuel Gomez-Rodriguez. Regression under human assistance. In *Proceedings of the AAAI Conference on Artificial Intelligence*, volume 34, pages 2611–2620, 2020.

[6] Yaroslav Ganin, Evgeniya Ustinova, Hana Ajakan, Pascal Germain, Hugo Larochelle, François Laviolette, Mario Marchand, and Victor Lempitsky. Domain-adversarial training of neural networks. *The journal of machine learning research*, 17(1):2096–2030, 2016.

[7] Moritz Hardt, Nimrod Megiddo, Christos Papadimitriou, and Mary Wootters. Strategic classification. In *Proceedings of the 2016 ACM conference on innovations in theoretical computer science*, pages 111–122, 2016.

[8] Moritz Hardt, Eric Price, and Nati Srebro. Equality of opportunity in supervised learning. In *Advances in neural information processing systems*, pages 3315–3323, 2016.

[9] Amir-Hossein Karimi, Gilles Barthe, Bernhard Schölkopf, and Isabel Valera. A survey of algorithmic recourse: definitions, formulations, solutions, and prospects, 2021.

[10] Sagi Levanon and Nir Rosenfeld. Strategic classification made practical. *arXiv preprint arXiv:2103.01826*, 2021.

[11] Arnaud Van Looveren and Janis Klaise. Interpretable counterfactual explanations guided by prototypes, 2019.

[12] Brian Lubars and Chenhao Tan. Ask not what ai can do, but what ai should do: Towards a framework of task delegability. *Advances in Neural Information Processing Systems*, 32, 2019.

[13] Spandan Madan, Tomotake Sasaki, Tzu-Mao Li, Xavier Boix, and Hanspeter Pfister. Small in-distribution changes in 3d perspective and lighting fool both cnns and transformers. *arXiv preprint arXiv:2106.16198*, 2021.

[14] David Madras, Toni Pitassi, and Richard Zemel. Predict responsibly: improving fairness and accuracy by learning to defer. *Advances in Neural Information Processing Systems*, 31, 2018.

[15] John Miller, Smitha Milli, and Moritz Hardt. Strategic adaptation to classifiers: A causal perspective. *CoRR*, abs/1910.10362, 2019.

[16] Baharan Mirzasoleiman, Ashwinkumar Badanidiyuru, Amin Karbasi, Jan Vondrák, and Andreas Krause. Lazier than lazy greedy. *arXiv preprint arXiv:1409.7938*, 2014.

[17] Hussein Mozannar and David Sontag. Consistent estimators for learning to defer to an expert. In *International Conference on Machine Learning*, pages 7076–7087. PMLR, 2020.

[18] Siddharth Nayak and Balaraman Ravindran. Reinforcement learning for improving object detection. In *European Conference on Computer Vision*, pages 149–161. Springer, 2020.

[19] George L Nemhauser, Laurence A Wolsey, and Marshall L Fisher. An analysis of approximations for maximizing submodular set functions-i. *Mathematical programming*, 1978.

[20] Nastaran Okati, Abir De, and Manuel Gomez-Rodriguez. Differentiable learning under triage, 2021.

[21] Godliver Owomugisha and Ernest Mwebaze. Machine learning for plant disease incidence and severity measurements from leaf images. In *2016 15th IEEE International Conference on Machine Learning and Applications (ICMLA)*, pages 158–163, 2016.

[22] Chunjong Park, Hung Ngo, Libby Rose Lavitt, Vincent Karuri, Shiven Bhatt, Peter Lubell-Doughtie, Anuraj H. Shankar, Leonard Ndwiga, Victor Osoti, Juliana K. Wambua, Philip Bejon, Lynette Isabella Ochola-Oyier, Monique Chilver, Nigel Stocks, Victoria Lyon, Barry R. Lutz, Matthew Thompson, Alex Mariakakis, and Shwetak Patel. The design and evaluation of a mobile system for rapid diagnostic test interpretation. *Proc. ACM Interact. Mob. Wearable Ubiquitous Technol.*, 5(1), mar 2021.

[23] Rafael Poyiadzi, Kacper Sokol, Raul Santos-Rodriguez, Tijl De Bie, and Peter Flach. Face: Feasible and actionable counterfactual explanations. In *Proceedings of the AAAI/ACM Conference on AI, Ethics, and Society*, AIES '20, page 344–350, New York, NY, USA, 2020. Association for Computing Machinery.

[24] Maithra Raghu, Katy Blumer, Greg Corrado, Jon Kleinberg, Ziad Obermeyer, and Sendhil Mullainathan. The algorithmic automation problem: Prediction, triage, and human effort. *arXiv preprint arXiv:1903.12220*, 2019.

[25] Alexis Ross, Himabindu Lakkaraju, and Osbert Bastani. Learning models for actionable recourse. In A. Beygelzimer, Y. Dauphin, P. Liang, and J. Wortman Vaughan, editors, *Advances in Neural Information Processing Systems*, 2021.

[26] Shai Shalev-Shwartz and Shai Ben-David. *Understanding machine learning: From theory to algorithms*. Cambridge university press, 2014.

[27] Jonathan Shen, Ruoming Pang, Ron J Weiss, Mike Schuster, Navdeep Jaitly, Zongheng Yang, Zhifeng Chen, Yu Zhang, Yuxuan Wang, Rj Skerrv-Ryan, et al. Natural tts synthesis by conditioning wavenet on mel spectrogram predictions. In *2018 IEEE international conference on acoustics, speech and signal processing (ICASSP)*, pages 4779–4783. IEEE, 2018.

[28] Rohan Taori, Achal Dave, Vaishaal Shankar, Nicholas Carlini, Benjamin Recht, and Ludwig Schmidt. Measuring robustness to natural distribution shifts in image classification, 2020.

[29] Berk Ustun, Alexander Spangher, and Yang Liu. Actionable recourse in linear classification. In *Proceedings of the Conference on Fairness, Accountability, and Transparency*, pages 10–19, 2019.

[30] S. Wachter, Brent D. Mittelstadt, and Chris Russell. Counterfactual explanations without opening the black box: Automated decisions and the gdpr. *European Economics: Microeconomics & Industrial Organization eJournal*, 2017.

[31] Bryan Wilder, Eric Horvitz, and Ece Kamar. Learning to complement humans. In *IJCAI*, 2020.

[32] Jiaming Zeng, Berk Ustun, and Cynthia . Interpretable classification models for recidivism prediction. *Journal of the Royal Statistical Society: Series A (Statistics in Society)*, 3(180):689–722, 2017.

[33] Ping Zhang, Rishabh Iyer, Ashish Tendulkar, Gaurav Aggarwal, and Abir De. Learning to select exogenous events for marked temporal point process. *Advances in Neural Information Processing Systems*, 34, 2021.

Checklist

1. For all authors...
   (a) Do the main claims made in the abstract and introduction accurately reflect the paper's contributions and scope? [Yes] See Section 3.2, 4
   (b) Did you describe the limitations of your work? [Yes] See Section 7

(c) Did you discuss any potential negative societal impacts of your work? [N/A]

(d) Have you read the ethics review guidelines and ensured that your paper conforms to them? [Yes]

2. If you are including theoretical results...

   (a) Did you state the full set of assumptions of all theoretical results? [Yes] See Section 3.2

   (b) Did you include complete proofs of all theoretical results? [Yes] Included in the Appendix.

3. If you ran experiments...

   (a) Did you include the code, data, and instructions needed to reproduce the main experimental results (either in the supplemental material or as a URL)? [Yes] Code is included in the Supplementary Material and datasets are provided in an anonymized URL.

   (b) Did you specify all the training details (e.g., data splits, hyperparameters, how they were chosen)? [Yes] See Section 4 and Appendix

   (c) Did you report error bars (e.g., with respect to the random seed after running experiments multiple times)? [Yes] See Section 4

   (d) Did you include the total amount of compute and the type of resources used (e.g., type of GPUs, internal cluster, or cloud provider)? [Yes] See Appendix

4. If you are using existing assets (e.g., code, data, models) or curating/releasing new assets...

   (a) If your work uses existing assets, did you cite the creators? [Yes]

   (b) Did you mention the license of the assets? [N/A]

   (c) Did you include any new assets either in the supplemental material or as a URL? [Yes] Datasets are included in an anonymized URL

   (d) Did you discuss whether and how consent was obtained from people whose data you're using/curating? [Yes]

   (e) Did you discuss whether the data you are using/curating contains personally identifiable information or offensive content? [N/A]

5. If you used crowdsourcing or conducted research with human subjects...

   (a) Did you include the full text of instructions given to participants and screenshots, if applicable? [N/A]

   (b) Did you describe any potential participant risks, with links to Institutional Review Board (IRB) approvals, if applicable? [N/A]

   (c) Did you include the estimated hourly wage paid to participants and the total amount spent on participant compensation? [N/A]

A Errata

Fixed in the revision.

B Proofs of technical results

B.1 Proof of Proposition 1

Proposition 1 *Assume that Z is $L_{\boldsymbol{\beta}}$-Lipschitz with respect to $\boldsymbol{\beta}$, the model $\log f_\theta(y \mid \mathbf{x})$ is L_x-Lipschitz with respect to $\mathbf{x}$. Given $i \in D$ and $j \in B_i$, if the set $\mathrm{Rec}_\Delta(\theta, \mathbf{x}_{ij}, y_i)$ is non-empty and the recourse network g_ϕ gives a modified $\boldsymbol{\beta}'_{ij}$ such that $||\boldsymbol{\beta}'_{ij} - \boldsymbol{\beta}|| \leq \epsilon$ for some $\boldsymbol{\beta} \in \mathrm{Rec}_\Delta(\theta, \mathbf{x}_{ij}, y_i)$, then, for $\Delta > tL_xL_{\boldsymbol{\beta}}\epsilon$ with $t > 1$ we have:*

$$\log f_\theta(y_i \mid Z(z_i, \boldsymbol{\beta}'_{ij})) > \log f_\theta(y_i \mid \mathbf{x}_{ij}) + (1 - 1/t)\,\Delta \tag{12}$$

Proof. Recall that by definition in Eq. (3) in our main submission,

$$\mathrm{Rec}_\Delta(\theta, \mathbf{x}, y) = \{\boldsymbol{\beta}' \mid \log f_\theta\left(Z(z_i, \boldsymbol{\beta}'), y\right) > \log f_\theta\left(y \mid \mathbf{x}\right) + \Delta\} \tag{13}$$

Thus, for $\boldsymbol{\beta}'_{ij} \in \mathrm{Rec}_\Delta(\theta, \mathbf{x}_{ij}, \boldsymbol{\beta}_{ij})$ we have,

$$\begin{aligned}
\log f_\theta(y_i \mid \mathbf{x}_{ij}) &< \log f_\theta(y_i \mid \mathbf{x}'_{ij} = Z(\mathbf{x}_{ij}, \boldsymbol{\beta}'_{ij})) - \Delta \\
&= \log f_\theta(y_i \mid Z(z_i, \boldsymbol{\beta})) + \log f_\theta(y_i \mid \mathbf{x}'_{ij} = Z(\mathbf{x}_{ij}, \boldsymbol{\beta}'_{ij})) \\
&\quad - \log f_\theta(y_i \mid Z(z_i, \boldsymbol{\beta})) - \Delta \\
&\overset{(1)}{<} \log f_\theta(y_i \mid Z(z_i, \boldsymbol{\beta})) + L_x||\mathbf{x}'_{ij} - Z(z_i, \boldsymbol{\beta})|| - \Delta \\
&= \log f_\theta(y_i \mid Z(z_i, \boldsymbol{\beta})) + L_x||Z(z_i, \boldsymbol{\beta}'_{ij}) - Z(z_i, \boldsymbol{\beta})|| - \Delta \\
&\overset{(2)}{<} \log f_\theta(y_i \mid Z(z_i, \boldsymbol{\beta})) + L_xL_{\boldsymbol{\beta}}\epsilon - \Delta \\
&\overset{(3)}{<} \log f_\theta(y_i \mid Z(z_i, \boldsymbol{\beta})) + (1/t - 1)\Delta
\end{aligned} \tag{14}$$

The inequality (1) is due to the L_x Lipschitz-continuity of $f_\theta(y \mid \mathbf{x})$ in $\mathbf{x}$. The inequality (2) is due to the $L_{\boldsymbol{\beta}}$ Lipschitz-continuity of $Z(z, \boldsymbol{\beta})$ in $\boldsymbol{\beta}$. The last inequality (3) follows from the assumption that $\Delta > tL_xL_{\boldsymbol{\beta}}\epsilon$.

B.2 Proof of Proposition 2

Proposition 2 *Let us assume that the true conditional distribution of y given $\mathbf{x}$ is f_{θ^*}, $\log f_\theta(y \mid \mathbf{x})$ is L_θ-Lipschitz w.r.t. θ and $||\theta - \theta^*|| \leq \delta$. Moreover, we define the following quantities:*

$$\Delta^{(i,j)} = \max_{r \in B_i} \left[\log f_{\theta^*}(y_i \mid \mathbf{x}_{ir}) - \log f_{\theta^*}(y_i \mid \mathbf{x}_{ij})\right] \tag{15}$$

$$A = \{(i,j) \in V \mid \Delta^{(i,j)} > 0\} \tag{16}$$

$$\Delta_0 = \min_{(i,j) \in A} \Delta_{i,j} \tag{17}$$

Then, we have the following results:

1. *For $(i,j) \in A$, $\mathrm{Rec}_{\Delta_0}(\theta^*, \mathbf{x}_{ij}, y_i)$ is non-empty.*
2. *Given $(i,j) \in V$, if we have $\delta < \frac{\Delta_0}{2L_\theta}$, then $\mathrm{Rec}_\Delta(\theta, \mathbf{x}_{ij}, y_i)$ is non-empty for $\Delta < \Delta_0 - 2L_\theta\delta$*
3. *If the recourse network g_ϕ gives us a modified $\boldsymbol{\beta}'_{ij}$ such that $||\boldsymbol{\beta}'_{ij} - \boldsymbol{\beta}|| \leq \epsilon$ for some $\boldsymbol{\beta} \in \mathrm{Rec}_\Delta(\theta, \mathbf{x}_{ij}, y_i)$ with $\Delta < \Delta_0 - 2L_\theta\delta$, then, for $\epsilon < (\Delta_0 - 2L_\theta\delta)/(tL_{\boldsymbol{\beta}}L_x)$ with $t > 1$, we have:*

$$\log f_\theta(y_i \mid \mathbf{x}_{ij}) < \log f_\theta(y_i \mid Z(z_i, \boldsymbol{\beta}'_{ij})) - (1 - 1/t)(\Delta^{(i,j)} - 2L_\theta\delta) \tag{18}$$

Proof. The statement (1) is true by definition.

$$\log f_\theta(y_i \mid \mathbf{x}_{ij}) = \log f_{\theta^*}(y_i \mid \mathbf{x}_{ij}) + \log f_\theta(y_i \mid \mathbf{x}_{ij}) - \log f_{\theta^*}(y_i \mid \mathbf{x}_{ij}) \tag{19}$$

$$\overset{(1)}{\leq} \log f_{\theta^*}(y_i \mid \mathbf{x} = Z(z_i, \boldsymbol{\beta})) + \log f_\theta(y_i \mid \mathbf{x}_{ij}) - \log f_{\theta^*}(y_i \mid \mathbf{x}_{ij}) - \Delta_0 \tag{20}$$

$$= \log f_\theta(y_i \mid \mathbf{x} = Z(z_i, \boldsymbol{\beta})) + \log f_{\theta^*}(y_i \mid \mathbf{x} = Z(z_i, \boldsymbol{\beta})) - \log f_\theta(y_i \mid \mathbf{x} = Z(z_i, \boldsymbol{\beta})) + \log f_\theta(y_i \mid \mathbf{x}_{ij}) - \log f_{\theta^*}(y_i \mid \mathbf{x}_{ij}) - \Delta_0 \tag{21}$$

$$\leq \log f_\theta(y_i \mid \mathbf{x} = Z(z_i, \boldsymbol{\beta})) - (\Delta_0 - 2L_\theta \delta) \tag{22}$$

Thus $\mathrm{Rec}_\Delta(\theta, \mathbf{x}_{ij}, y_i)$ is non-empty for $\Delta < \Delta_0 - 2L_\theta\delta$. Next, we have

$$\begin{aligned}
&\log f_\theta(y_i \mid \mathbf{x} = Z(z_i, \boldsymbol{\beta})) - (\Delta_0 - 2L_\theta\delta) \\
&= \log f_\theta(y_i \mid \mathbf{x}'_{ij} = Z(z_i, \boldsymbol{\beta}'_{ij})) \\
&\quad + \log f_\theta(y_i \mid \mathbf{x} = Z(z_i, \boldsymbol{\beta})) - \log f_\theta(y_i \mid \mathbf{x}'_{ij} = Z(z_i, \boldsymbol{\beta}'_{ij})) - (\Delta_0 - 2L_\theta\delta) \\
&\leq \log f_\theta(y_i \mid \mathbf{x}'_{ij} = Z(z_i, \boldsymbol{\beta}'_{ij})) + L_x L_\beta \epsilon - (\Delta_0 - 2L_\theta\delta)
\end{aligned} \tag{23}$$

The last inequality is due to the Lipschitzness of f_θ with respect to $\mathbf{x}$, the Lipschitzness of Z with respect to $\boldsymbol{\beta}$; and, $||\boldsymbol{\beta}_{ij} - \boldsymbol{\beta}|| \leq \epsilon$.

B.3 Analysis of our greedy algorithm

We first start with an assumption that $\log f_\theta$ is algorithmically stable, *i.e.*, if it is trained upon a dataset V of size N, then $||\theta^*(V) - \theta^*(V')|| < \frac{\rho}{N}$, where $|V \backslash V'| = |V' \backslash V| = 1$, *i.e.*, V and V' has $N-1$ elements in common and therefore, V' is obtained by replacing one element of V. It is well known that minimizing regularized convex and L-Lipschitz loss functions are stable with $\rho = 2L/\lambda_{\min}$ where $\lambda_{\min}$ is the minimium eigenvalue of the regularized convex loss [26, Chapter 13, Regularization and stability]. For Polyak-Lojasiewicz (PL) loss functions with PL-coefficient μ [4, corollary 4], we have $||\theta^*(V) - \theta(V')|| < \frac{2L^2}{\mu(N-1)} \leq \frac{4L^2}{\mu N}$ for $N > 2$. Under this assumption, we state the following result:

Proposition 3 *Suppose,* $\log f_\theta$ *is stable,* i.e., $||\theta^*(V) - \theta^*(V')|| < \frac{\rho}{N}$ *for some constant* ρ *where* V' *is obtained by replacing one element of* V*. Then, let us assume that the true conditional distribution of* y *given* $\mathbf{x}$ *is* f_{θ^*}*,* $\log f_\theta(y \mid \mathbf{x})$ *is* L_θ*-Lipschitz w.r.t.* θ*. Moreover, we define the following quantities:*

$$\Delta^{(i,j)} = \max_{r \in B_i} [\log f_{\theta^*}(y_i \mid \mathbf{x}_{ir}) - \log f_{\theta^*}(y_i \mid \mathbf{x}_{ij})] \tag{24}$$

$$A = \{(i,j) \in V \mid \Delta^{(i,j)} > 0\} \tag{25}$$

$$\Delta_0 = \min_{(i,j) \in A} \Delta_{i,j} \tag{26}$$

Now, note that if $(i,j) \in A$*, then it is obvious that* $\mathrm{Rec}_{\Delta_0}(\theta^*, \mathbf{x}_{ij}, y_i)$ *is non-empty. Assume that* $|A| > b$*,* $||\theta(R^{(0)}) - \theta^*|| < \delta < \frac{\Delta_0}{2L_\theta}$ *and* $|V|$ *is large enough so that* $|V| > \frac{2L_\theta \rho b}{\Delta_0 - 2L_\theta \delta}$ *Now if* $R^{(k)}$ *is solution in* R *during the* k*-th iteration of our greedy algorithm, then the greedy algorithm will choose* (i,j) *at each step* $k \in \{1, .., b\}$ *so that*

$$F(\theta^*(R^{(k)} \cup (i,j)), R^{(k)} \cup (i,j)) > F(\theta^*(R^{(k)}), R^{(k)}) \tag{27}$$

when $0 < \Delta < \Delta_0 - 2L_\theta \left(\delta + \frac{\rho b}{|V|}\right)$.

Proof. Assume that during k-th iteration, we have the following snapshot of the training instances:

$$V^{(k)} = \{\underbrace{(\mathbf{x}_{i_1,j_1}, y_1), \ldots, (\mathbf{x}_{i_m,j_m}, y_m)}_{V \backslash R^{(k)}}, \underbrace{(\mathbf{x}'_{i_1,j_1}, y'_1), \ldots, (\mathbf{x}'_{i_a,j_a}, y'_a)}_{\text{Instances after applying recourse on } R^{(k)}}\} \tag{28}$$

We add *atmost* one element (i,j) to $R^{(k)}$ to obtain $R^{(k+1)}$. This can be seen as replacing atmost one instance (i,j) in V with a new instance obtained after applying recourse on (i,j). As the model is

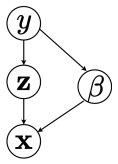

Figure 9: Causal Model that depicts the data generating process of human.

stable, then we have:

$$||\theta^*(R^{(k+1)}) - \theta^*(R^{(k)})|| \leq \frac{\rho}{|V|} \tag{29}$$

Since we start with $||\theta^*(R^0) - \theta^*|| \leq \delta$, by consecutively applying triangle inequalities, we have:

$$||\theta^*(R^k) - \theta^*|| \leq \delta + \frac{\rho k}{|V|} \leq \delta + \frac{\rho b}{|V|} \tag{30}$$

Now, from the first part of Proposition 2, we show that, whenever $\mathrm{Rec}_{\Delta_0}(\theta^*, \mathbf{x}_{ij}, y_i)$ is non-empty with $\Delta_0 > 2L_\theta \left(\delta + \frac{\rho b}{|V|}\right)$, then $\mathrm{Rec}_{\Delta}(\theta^*(R^{(k)}), \mathbf{x}_{ij}, y_i)$ is nonempty for $\Delta < \Delta_0 - 2L_\theta \left(\delta + \frac{\rho b}{|V|}\right)$. Hence, there will be b instances for which $\mathrm{Rec}_{\Delta}(\theta^*(R^{(k)}), \mathbf{x}_{ij}, y_i)$ is non-empty. Now we have:

$$\begin{aligned}
&F(\theta^*(R^{(k)} \cup (i,j)), R^{(k)} \cup (i,j)) - F(\theta^*(R^{(k)}), R^{(k)}) \\
&\quad = F(\theta^*(R^{(k)} \cup (i,j)), (R^{(k)} \cup (i,j))) - F(\theta^*(R^{(k)}), R^{(k)} \cup (i,j)) \\
&\qquad + F(\theta^*(R^{(k)}), R^{(k)} \cup (i,j)) - F(\theta^*(R^{(k)}), R^{(k)}) \\
&\quad \overset{(1)}{\geq} F(\theta^*(R^{(k)}), R^{(k)} \cup (i,j)) - F(\theta^*(R^{(k)}), R^{(k)})
\end{aligned} \tag{31}$$

Inequality (1) is due to the fact that: $F(\theta^*(R^{(k)} \cup (i,j)), (R^{(k)} \cup (i,j))) \geq F(\theta^*(R^{(k)}), R^{(k)} \cup (i,j))$. Now given this element (i,j), we will choose it for recourse if $\mathrm{Rec}_{\Delta}(\theta^*(R^{(k)}), \mathbf{x}_{ij}, y_i)$ is non-empty.

Now since there are at least b elements for which $\mathrm{Rec}_{\Delta}(\theta^*(R^{(k)}), \mathbf{x}_{ij}, y_i)$ is non-empty, we will find at least $b - k$ elements which would be chosen for recourse at this k-th step. For those elements, we will have $\boldsymbol{\beta}_{ir} \in \mathrm{Rec}_{\Delta}(\theta^*(R^{(k)}), \mathbf{x}_{ij}, y_i)$ and then we have:

$$F(\theta^*(R^{(k)}), R^{(k)} \cup (i,j)) - F(\theta^*(R^{(k)}), R^{(k)}) = \log f_\theta(y_i \,|\, \mathbf{x}_{ir}) - \log f_\theta(y_i \,|\, \mathbf{x}_{ij}) > 0 \tag{32}$$

Thus, there will be at least $b - k$ elements for which

$$F(\theta^*(R^{(k)} \cup (i,j)), R^{(k)} \cup (i,j)) - F(\theta^*(R^{(k)}), R^{(k)}) > 0 \tag{33}$$

Since, we choose (i,j) to be the one with highest gain, we conclude that, for any step $k \leq b$, the instance (i,j) chosen for recourse, the underlying gain would be strictly positive.

C Additional details about experimental setup

Causal Model. The causal model that depicts the relationships between the variables $\mathbf{x}, \boldsymbol{\beta}, y, z$ in our dataset is shown in the Figure 9

Synthetic Dataset. We generate a 4 class synthetic real valued dataset with $|D| = 1200$ objects $z_i \in \mathcal{Z} = R^{d_z}$ with $d_z = 6$. The objects z_i are sampled from class dependent Isotropic Gaussian distribution $\mathcal{N}(\mu_y, \Sigma_y)$ where $\Sigma_y = \mathrm{Diag}[0.1, 0.25, 0.1, 0.1, 0.25, 0.1]$ for all $y \in \mathcal{Y}$. The means $\mu_0 = [-1,\ 0,\ 0.5,\ 0.5,\ 0,\ 0], \mu_1 = [1,\ 0,\ 0.5,\ 0.5,\ 0,\ 0], \mu_2 = [0,\ -1,\ 0,\ 0,\ -0.5,\ -0.5], \mu_3 = [0,\ 1,\ 0,\ 0,\ -0.5,\ -0.5]$. Then, we draw $\boldsymbol{\beta}_{ij} \sim \mathrm{Unif}\{0,1\}^{d_z}$ such that they have exactly 3 bits set to 1 and none of them have both $\boldsymbol{\beta}_{ij}[0] = \boldsymbol{\beta}_{ij}[1] = 1$. Finally, we set $\mathbf{x}_{ij} = z_i \odot \boldsymbol{\beta}_{ij}$ for $i \in D$ and $j \in B_i$ where $|B_i| = 8$. The purpose of g_ϕ thus is to predict which bits in the input should be unmasked so as to make f_θ predict the correct label.

Generating Shapenet Datasets. As mentioned in our main submission, we work with two versions of Shapenet dataset namely Shapenet-Large and Shapenet-Small which differ in the group size $|B_i|$. While Shapenet-Large has 4 renderings for each z_i, Shapenet-Small has only 2 rendering for each z_i. Recall that we corrupt certain $\mathbf{x}_{ij}$ if $\boldsymbol{\beta}_{ij}$ used to render them is inherently noisy. Here, we expand more on how we inject noise. We use imagecorruptions python li-

Class	front view zoom in yellow	front view normal zoom white	top view zoom in yellow	left&side zoom out pink	left&side normal zoom white	front&top normal zoom white	front&top zoom out green	side&top zoom out pink	side&front zoom out yellow
Aeroplane	✓		✓	✓	✓		✓	✓	✓
Bench	✓	✓					✓		✓
Bus		✓				✓	✓	✓	✓
Cabinet									✓
Chair									
Display									
Knife		✓							✓
Lamp	✓			✓		✓	✓		✓
Speaker									
Gun	✓	✓	✓		✓	✓	✓	✓	

Table 10: This table denotes the classes that admit noisy $\boldsymbol{\beta}$. ✓ indicates that images having the corresponding $(y, \boldsymbol{\beta})$ are corrupted w.p. 0.5. We picked $(\boldsymbol{\beta}, y)$ pairs through visual inspection and decided to corrupt a random subset of them so as to make the learning task more challenging for f_θ thereby amplifying the need for recourse.

brary[5] for injecting noise to $\mathbf{x}_{ij}$. It provides us API for 15 different types of noise. We selected 9 of them namely {`gaussian_noise, shot_noise, impulse_noise, frost, fog, brightness, elastic_transform, pixelate, jpeg_compression`}. Each of these APIs accept an RGB image as input and outputs an RGB image with noise added to it. For each label y, we select a set of $\boldsymbol{\beta}$s so that any image generated under these settings $(\boldsymbol{\beta}, y)$ will be noisy with certain probability. Let us denote this set of noisy $\boldsymbol{\beta}$ for a given y as $\boldsymbol{\beta}_y^{noise}$. Once we obtain $y_i, \boldsymbol{\beta}_{ij}, z_i$ following the sampling procedure depicted by the Figure 9, we render the corresponding $\mathbf{x}_{ij}$ under one of the following two cases: (a) if $\boldsymbol{\beta}_{ij} \in \boldsymbol{\beta}_{y_i}^{noise}$, we render $\mathbf{x}_{ij}$ in a noisy manner w.p. 0.5 *i.e.* we subject the image rendered using $(\boldsymbol{\beta}_{ij}, z_i)$ to one of the 9 noises selected uniformly at random thereby rendering a noisy $\mathbf{x}_{ij}$. (b) if $\boldsymbol{\beta}_{ij} \notin \boldsymbol{\beta}_{y_i}^{noise}$, we simply render $\mathbf{x}_{ij}$ in the setting $(\boldsymbol{\beta}_{ij}, z_i)$ without adding any noise to it.

Generating Speech Commands Dataset. For this dataset, we choose 20 commands with $\mathcal{Y} =$ {`cancel`, `disable`, `enable`, `decrease`, `increase`, `good morning`, `good night`, `lock`, `open`, `door`, `pauseplay`, `set`, `show`, `skip`, `snooze`, `start`, `stop`, `turn off`, `turn on`}. We chose rhyming words so as to make the classification task harder. Unlike Shapenet, we decided to embed noise in sample generation as part of $\boldsymbol{\beta}$ itself so as to simulate real life scenarios. Because we work with Mel spectograms (images), we fixed the model architecture for f_θ, g_ϕ to be the same as that of Shapenet.

Generating Skin Lesion Dataset. This dataset consists of images of skin captured using smartphone and the task is to predict different skin conditions ($|\mathcal{Y}| = 7$) namely {`melanocytic nevi` , `melanoma`, `basal cell carcinoma`, `actiniv keratoses an`, `vascular lesions`, `benign keratoses lik`, `dermatofibroma`}. The dataset is taken from from Kaggle [6] and synthetically generated environments. We generate images under 9 different environments ($|\mathcal{B}| = 9$) where each environment is defined by (zoom, illumination, contrast). For zoom, we assume that the original image is at 100% zoom level and create two additional zoom levels namely $175\%, 250\%$. For illumination, we chose three values to simulate the impact of a skin image captured in light, dark, and the original image. For contrast also we chose three values and simulated low, normal and high contrast skin images. We fixed the model architecture for f_θ, g_ϕ to be the same as that of Shapenet.

D Results on Synthetic Dataset

Here, we compare the performance of various recourse trigger and recourse recommender methods on the synthetic dataset. We summarize the results in Figure 11 — we make the following observations. (1) Since the generated dataset is not linearly separable, the accuracy of f_θ is 77%. Moreover, the greedy algorithm for training f_θ improves the accuracy by 3% over a model that trains on all data. (2) The accuracy provided by both recourse trigger π and recourse recommender g_ϕ improves as we

[5] https://github.com/bethgelab/imagecorruptions

[6] `https://www.kaggle.com/code/kmader/deep-learning-skin-lesion-classification/notebook`

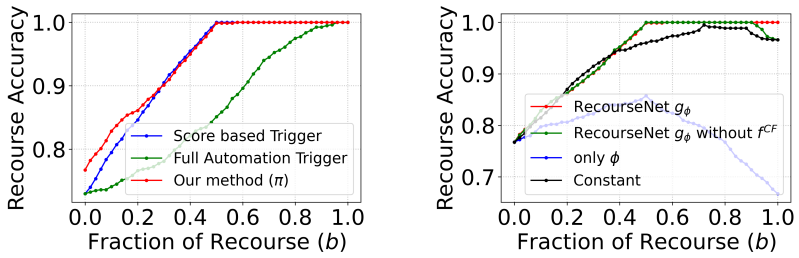

(a) Recourse trigger π (b) Recourse recommender g_ϕ

Figure 11: Recourse accuracy vs recourse fraction *i.e.* maximum instances that can undergo recourse for Synthetic dataset. Panel (a) shows performance comparison of recourse trigger π with baselines. Panel (b) shows performance comparison of recourse recommender g_ϕ with a constant predictor.

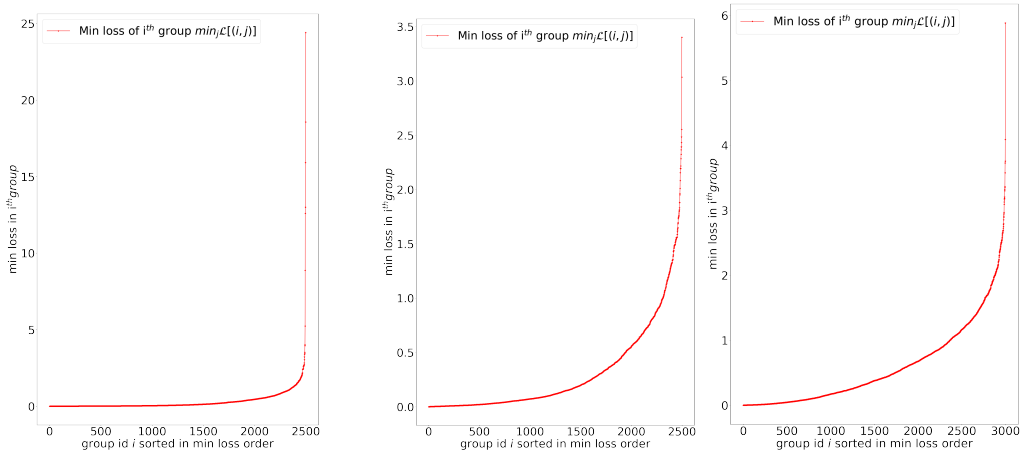

(a) Shapenet-Large (b) Shapenet-Small (c) Speech-Commands

Figure 12: This shows the min loss in each group in a sorted order. We use this to select the groups into D_δ. As discussed in the main submission, the groups in D_δ have atleast one good feature and thus its min loss must be very close to 0. In this view, we set D_δ = the first 1800 min loss groups for Shapenet-large and the first 1250 min loss groups for shapenet-small. For Speech commands we set the first 1400 groups as part of the set D_δ.

increase b. We notice in the dataset that it is necessary to have 1^{st} bit unmasked for instances labelled $\{y = 0, y = 1\}$ and 2^{nd} bit unmasked for the classes $\{y = 2, y = 3\}$ so that f_θ can predict them correctly. Our g_ϕ is able to learn this pattern using cues from the remaining bits as expected. (3) We observe a linear trend in improvement until about 48%; beyond which we observe a flat trend at 100% recourse accuracy. This is because $\boldsymbol{\beta}$ are randomly generated which leaves us with $\approx 50\%$ bad instances that require recourse. Only ϕ performs poorly because of arbitration in the supervision provided by the pseudo labels that are committed while training. The model has no flexibility to pick and choose alternative good $\boldsymbol{\beta}$s in accordance with g_ϕ for instances where $\boldsymbol{\beta}$ prediction becomes hard. (4) Constant prediction on the other hand fails to emit instance specific recourse recommendation and hence suffers to improve the recourse accuracy consistently.

E Models and Hyper-parameters

Moved to the main paper

F Additional Baselines

We added new baselines to compare with RECOURSENET. In all these we train f_θ on the entire training dataset but instead of g_ϕ we learn networks that estimate accuracy of an input $\mathbf{x}_{ij}$ on a counter-

Figure 13: This figure shows renderings of a chair object under different $\boldsymbol{\beta}$s. Each $\boldsymbol{\beta}$ is a 3-tuple namely *(view, zoom-level, light color)*.

factual setting $\boldsymbol{\beta}$ using ideas from the domain-invariant representations and Individual Treatment Effect estimation literature. **(1) Domain Adversarial Neural Network based training.** This method [6] aims to learn domain invariant representations using GANs based minmax objective. We extract representations of input ($\mathbf{x}$) by fine tuning a Resnet18 model with pre trained Imagenet weights. Then from the representation layer, we spawn a domain classifier that predicts the environment $\boldsymbol{\beta}$ that generated the instance $\mathbf{x}$. We multiply $\mathbf{x}$ representation with a domain reversal layer before feeding it to the domain classifier. The representations are concatenated with environment embedding and then fed to one more Fully connected Network that is spawned out of the representation layer. This network aims to predict classifier's confidence ($f_\theta(y|\mathbf{x})$) on the examples. **(2) TARNET.** We extract representations of input ($\mathbf{x}$) by fine tuning a Resnet18 model with pre-trained Imagenet weights. From the representation layer, we spawn $|\mathcal{B}|$ fully connected layers for each $\beta \in \mathcal{B}$. Each layer is thus responsible to predict classifier's confidence ($f_\theta(y|\mathbf{x})$) on only those instances that belong to the same environment β.
For Triage, since these methods directly model the counterfactual accuracy $P(y|\mathbf{x}, \boldsymbol{\beta})\forall\boldsymbol{\beta}$, we use these predicted values in place of our prior f^{CF} term in Eq (9). The results for these baselines in shown in the Figure 14. Our proposal beats all the baselines thus establishing the supremacy of out three-stage proposal for training RECOURSENET.

G Illustration of original and recoursed skin images

In this experiment, we visualize the original and recoursed images for the first five images in the Skin-Lesion test dataset that require recouse as per our triage policy. The visualizations are shown in the Figure 15. The images on the left are the test images before recourse and those on the right are the corresponding images that are obtained after recourse.

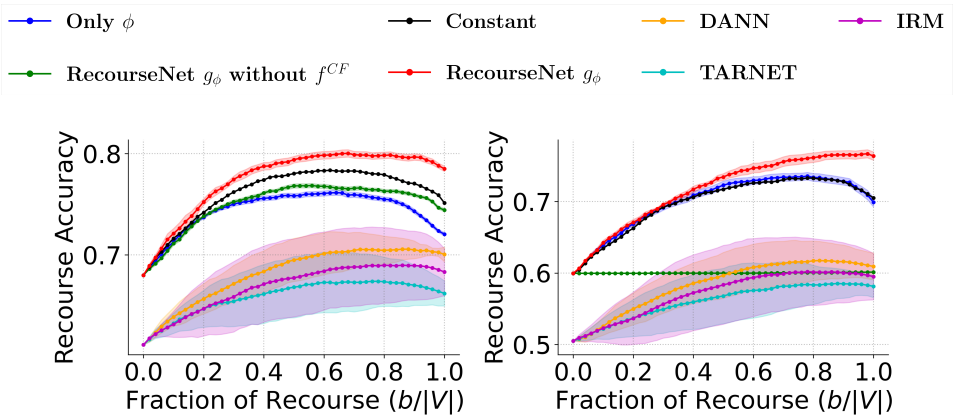

(a) Shapenet-Large

(b) Shapenet-Small

(c) Speech-Commands

(d) Skin-Lesion

Figure 14: This figure shows the performance of Recourse Recommender on all 4 datasets with newly added random baselines namely Invariant Risk Minimization, TARNET and Domain Adversarial Neural Network. The curves depict the mean Recourse accuracy $\pm$ one standard deviation over the mean for results obtained over five seeds.

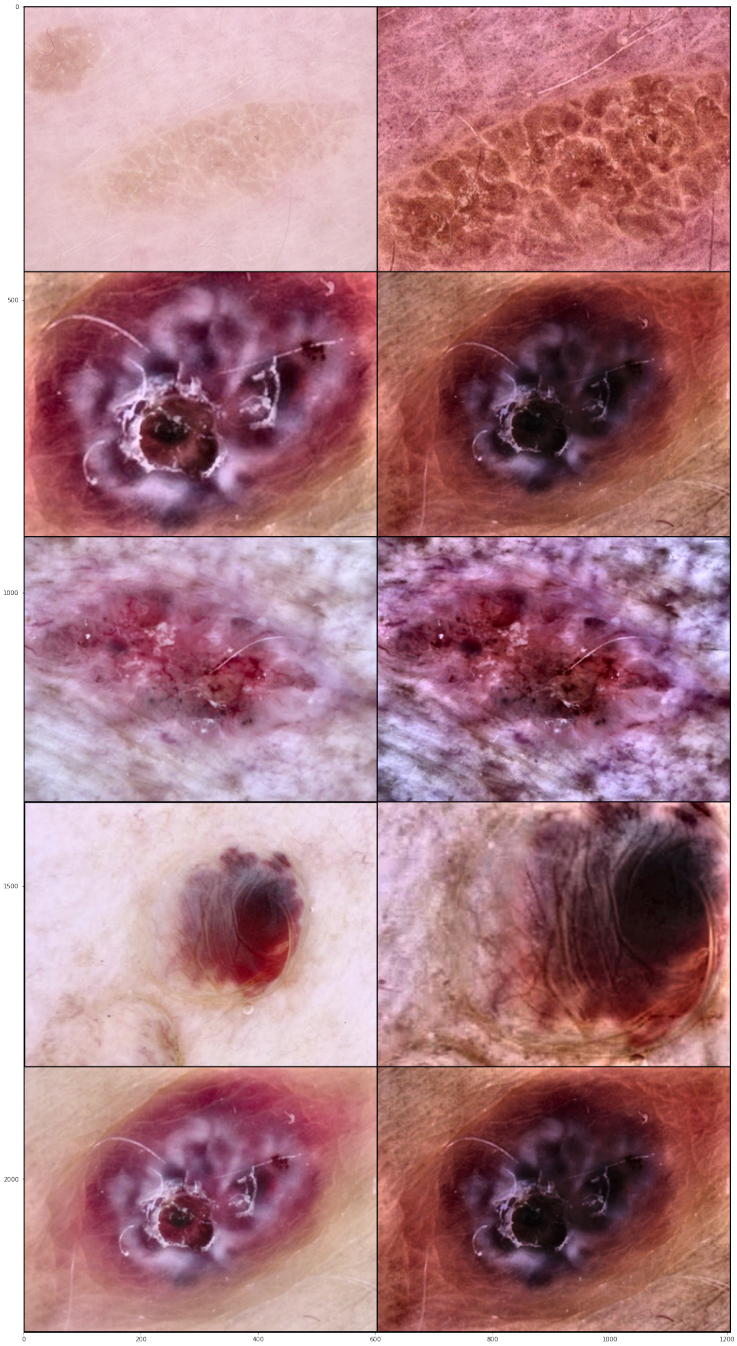

Figure 15: This figure shows the test images of the Skin-Lesion dataset before (left) and after recourse (right).